Pis'ma v ZhETF, vol.66, iss.2, pp.91 - 96 © 1997 July 25

SHOCK WAVE STRUCTURE IN DENSE GASES

V.V.Zhakhovskii[1)], *K.Nishihara*[*], *S.I.Anisimov*[**]

Institute for High Temperatures, RAS
127412 Moscow, Russia

[*]*Institute of Laser Engineering, Osaka University*
565 Osaka, Japan

[**]*Landau Institute for Theoretical Physics, RASciences*
117940 Moscow, Russia

Submitted 6 June 1997
Resubmitted 26 June 1997

Internal structure of shock wave front in a gas is studied using molecular dynamics (MD) simulation method. A new approach to MD shock simulation is used, which enables to consider a stationary shock front at rest and radically improves the quality of simulation. The profiles of flow variables and their fluctuations are calculated. The evolution of the velocity distribution function across the shock layer is calculated and compared with the bimodal distribution. The pair distribution function in the shock layer is determined. The surface tension associated with the shock wave is estimated.

PACS: 47.40.Nm, 47.45.-n, 51.10.+y

The shock wave is a principal element of gas-dynamics flows. Since the changes of flow parameters across a shock wave front are uniquely determined by the conservation laws and do not depend on the internal structure of the front, the shock wave is considered in gas dynamics as a structureless discontinuity. In the kinetic theory, the shock wave is treated as a transition layer of finite thickness, and its internal structure attracts particular interest. A major part of shock wave structure studies has been performed either in the hydrodynamic approximation [1-3] (which is valid for weak shocks), or on the basis of the Boltzmann kinetic equation (which holds for low density gases [4-9]). First gas kinetic analysis of strong shock wave structure was carried out in [4,5] using the so-called bimodal approximation. It is assumed that the distribution function within the wave may be represented as a linear combination of two Maxwellian distributions corresponding to uniform upstream and downstream flows:

$$f(\mathrm{v}, z) = (1 - \alpha(z))f_1(\mathrm{v}) + \alpha(z)f_2(\mathrm{v}) \qquad (1)$$

where $f_i(\mathrm{v})$ is the Maxwellian distribution with the particle number density n_i, the mass velocity u_i and the temperature T_i $(i = 1, 2)$. The subscripts 1 and 2 denote the uniform upstream and downstream conditions, respectively. The distribution function (1) does not satisfy the Boltzmann equation. Various equations have been proposed in the literature [7] to determine $\alpha(z)$. A comparison with experimental data shows reasonable accuracy of the bimodal approximation (1), but gives no way to choose, which of the equations proposed in the literature yields better results. Note that some of the results concerning the shock front structure obtained using the Boltzmann equation are in conflict with those obtained in the frame

[1)] e-mail: basil@landau.ac.ru

of hydrodynamics equations. For example, in the hydrodynamic approximation [1] the density approaches exponentially its limiting values, n_1 and n_2, as $|z| \to \infty$, whereas the solution of the Boltzmann equation for weak shock wave [10,11] shows a different asymptotic behavior. It is conceivable that this discrepancy might be attributed to the fact that only two-particle collisions are taken into account in the Boltzmann equation.

To calculate the shock front structure in solids, liquids, and dense gases the molecular dynamics method and the direct simulation Monte Carlo approach have been employed [9,12-15]. These simulation works have, however, several shortcomings. In the major part of MD simulations, a plane shock wave is generated by a piston compressing a fluid which is initially at rest. The resulting shock wave is unsteady. This approach, along with small number of particles in the simulation box, leads to unduly high level of nonphysical fluctuations [12-14]. As a result, there is no way to calculate the velocity distribution function within the shock front with sufficient accuracy. In Ref.[14], for example, qualitative statements concerning anisotropy and non-Maxwellian character of the velocity distribution inside the shock front are based on the calculation of the moments of the velocity distribution. Notice that the interpretation of the simulation results in [12-15] and other similar works is carried out usually in terms of hydrodynamics variables, some of which lose their meaning on a molecular scale.

In this work several physical problems related to the internal structure of shock waves are solved. First, we calculated local velocity distributions at several points within the shock front. Second, we found the asymptotic behavior of hydrodynamic variables in the shock wave. Third, we calculated an additional pressure resulting from shock front curvature (the effect similar to the surface tension). We consider a shock front which is at rest in a laboratory frame. A special potential configuration is used which accelerates the gas at one side of the MD cell and decelerates it at the opposite side. As a result, a stationary shock wave is formed inside the cell, and the level of fluctuations significantly decreases, as will be shown below.

We describe the interaction of atoms by the Lennard – Jones potential: $U(r) = 4\varepsilon[(\sigma/r)^{12} - (\sigma/r)^6]$. We will use the MD units determined in standard way [16] through the values of ε and σ. The rectangular MD cell $L_x \times L_y \times 2L_z$, has dimensions $56 \times 56 \times 240$ units. Total number of particles is 32000. The flow velocity $v(z) < 0$ is directed along the z-axis. Periodic boundary conditions are imposed along the three coordinate axes. The short-range potentials U^+ and U^- are located at $z = \pm L_z$ and satisfy the condition that the forces $\partial U^+/\partial z = \partial U^-/\partial z = 0$. Since the accelerating U^+ and decelerating U^- potentials have different magnitudes, the particles crossing the boundary $z = \pm L_z$ change their energy.

To form a uniform upstream flow with given temperature T_1 and mass velocity v_1, the Langevin thermostat [17] is used. The thermostat constitutes a part of MD cell (located in the $100 < z < 116$), in which the atoms are subjected to Langevin force

$$F_k^a(t) = R_k^a(t) - \beta(v_k^a - v_1\delta_{kz}) \qquad (2)$$

where the subscript $k = x, y, z$, the superscript a numbers atoms, β is the friction coefficient, and $R_k^a(t)$ is Gaussian random force. To obtain a prescribed temperature T_1, the parameters of Eq.(2) should satisfy the condition $\langle R^2 \rangle = 2\beta T_1/\Delta t$, where Δt is the time step of integration. The equations of motion are integrated using

the 8-th order Stoermer method. The details of the algorithm are described in [18]. The accuracy of calculations may be characterized by the relative amplitude of fluctuations of the total energy and center-of-mass position. In our calculations these amplitudes were less than 0.5%.

Going to the discussion of the results of simulations, we consider a typical case of moderate intesity shock wave (the Mach number $M = 12v_1/\sqrt{5}T_1 \approx 5.4v_1$) in moderate density gas. The parameters of shock waves at Mach numbers 2.65 and 8.19 are specified as:

$$\begin{array}{lllll} \text{(a)} & v_1 = -0.49, & n_1 = 0.0235, & T_1 = 0.992, \\ & v_2 = -0.181, & n_2 = 0.0632, & T_2 = 2.97; \end{array}$$

$$\begin{array}{lllll} \text{(b)} & v_1 = -1.50, & n_1 = 0.0235, & T_1 = 0.983, \\ & v_2 = -0.42, & n_2 = 0.0837, & T_2 = 19.96. \end{array}$$

The interatomic distance and the mean free path of atoms in the upstream flow are of the same order of magnitude: $d_1 \approx 3.5$ and $\lambda_1 \approx 6.4$ in the case (b). The parameters of uniform supersonic and subsonic flow satisfy the Hugoniot equation calculated using the equation of state data for argon taken from [19].

The number density profile within the shock front is shown in Fig.1. The shock wave thickness defined as $\delta = (n_2 - n_1)/|dn/dz|_{max}$ is in agreement with experimental data cited in in [14]. As noted above, in hydrodynamic approximation the differences $n(z) - n_1$ and $n_2 - n(z)$ decrease exponentially as $|z| \to \infty$. The analysis based on the Boltzmann equation [10,11] suggests that the above differences are proportional to $\exp(-k|z|^m)$ with $m < 1$. It follows from the results of simulation that $m = 1.01 \pm 0.03$. This result can be cosidered as an evidence that the kinetic approach [10,11] is not applicable to the description of asymptotic behavior of flow variables at $|z| \to \infty$. It would be instructive, however, to compute the exponent m using a larger MD cell.

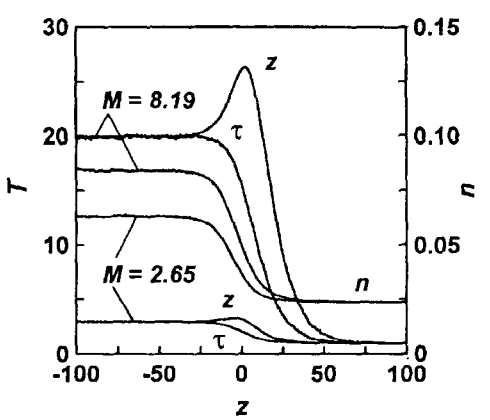

Fig.1. Density profiles in the shock front (n) and mean-square fluctuations of the longitudinal (z) and transverse (τ) molecular velocity components

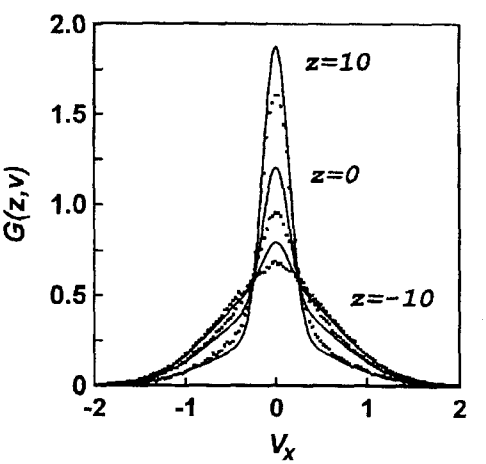

Fig.2. Variation of the velocity distribution functions $G_d(z, v_x)$ and $G_b(z, v_x)$ in the shock front at $M = 8.19$

The temperature profiles inside the shock front shown in many works make no physical sense because the temperature is not defined for nonequilibrium states. The value that is well defined is the mean square fluctuation of particle velocity (which is equal to the temperature in equilibrium). The simulation reveals that the fluctuations of the longitudinal (v_z) and transverse (v_x, v_y) velocity components show quite different behavior (Fig.1). When moving in the direction from upstream toward downstream, the fluctuation $\langle (v_z - \overline{v_z})^2 \rangle$ first rapidly increases, then passes through a maximum, and approaches its downstream value from above. The fluctuation $\langle v_x^2 \rangle$ increases more slowly and monotonically from its upstream to downstream value. To understand this behavior we note that the transformation of the energy of ordered motion along the z- axis into the energy of random motion along the x- axis requires large-angle scattering, which occurs when the particle velocity is large. Therefore, this process leads primarily to the generation of high energy tails in the distributions of particles over v_x and v_y, and the rate of the energy transformation is rather low. The randomization of the z-component of velocity is not much connected with the tails of distribution function and has a higher rate.

The evolution of the particle distributions over the velocity components inside the shock front is shown in Figs.2 and 3. The distribution functions are defined as

$$F(z, v_z) = \int f(z, \mathrm{v}) dv_x dv_y, \qquad G(z, v_x) = \int f(z, \mathrm{v}) dv_y dv_z.$$

The results of simulation (dots, subscript d) are compared with the bimodal distribution (1) (solic. lines, subscript b) for different thin layers normal to the z-axis. All distribution functions are normalized to unity. As is seen from Fig.2, the evolution of the v_x- distribution begins with the generation of high energy tails. Then the change is extended into the region of smaller v_x. In the vicinity of the point $v_x = 0$ the distribution remains unchanged until a new equilibrium state is reached. The bimodal approximation describes the evolution of the function $G(z, v_x)$ with a good accuracy.

The transformation of the v_z-distribution begins in a similar way: first, the high energy tail is formed. Then the new (downstream) distribution is formed due to the particle flux in the velocity space. It is seen from the results of simulation that the width of the distribution function $F(z, v_z)$ within the shock front is greater than its width in the equilibrium downstream flow. The function $F_b(z, v_z)$ calculated using the bimodal approximation (1) differs little from the function $F_d(z, v_z)$ obtained from the MD simulation. Calculations show, however, that the difference decreases with the Mach number decreasing. This fact is inconsistent with popular point of view that the bimodal distribution affords better approximation at higher Mach numbers when the shock wave thickness is small. At Mach numbers M close to unity, the functions $f_1(\mathrm{v})$ and $f_2(\mathrm{v})$ are close to each other, and Eq.(1) has correct limit as $M \to 1$. Fig.1-3 clarify the origin of the "temperature maximum" observed in some of the previous studies of shock wave structure, and show that the bimodal distribution (1) is close to the real distribution function in shock waves.

In Fig.4 the evolution of the pair distribution function $N(r)$, defined similarly to [16] (here r is the vector in the xy-plane) across the shock front is shown. In the upstream flow $N(r)$ reveals the maximum whose position corresponds to the minimum of the interparticle potential $r = 2^{1/6} \approx 1.12$. This maximum is less

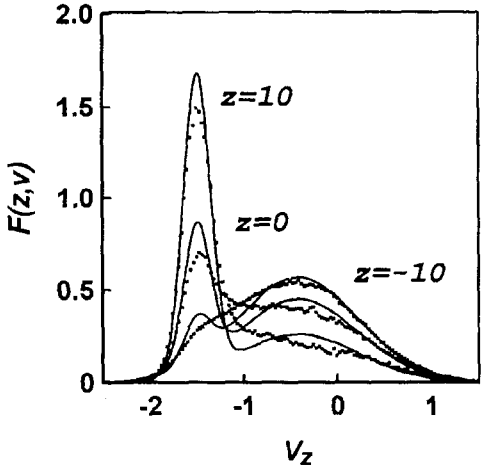

Fig.3. Variation of the velocity distribution functions: $F_d(z, v_z)$ and $F_b(z, v_z)$ in the shock front at $M = 8.19$

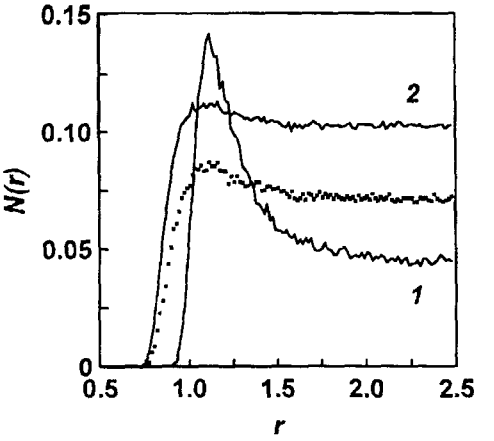

Fig.4. The pair distribution function in the upstream (1) and downstream (2) flows, and in the center of shock layer (dots) at $M = 8.19$

pronounced (but its position does not change) in the downstream flow, where the temperature is much greater than the potential minimum depth, ε. Correspondingly, the average potential energy per particle is about -0.2 in the upstream region and $+0.007$ in the downstream region.

Within the shock wave front, the velocity distribution function is not spherically symmetric. The pressure in this case is a symmetric tensor, rather than a scalar. The definition of this tensor in general nonequilibrium case is given in [20]. If the shock layer is planar (and normal to the z-axis), the pressure has diagonal form: $P_{xx} = P_{yy} = P_\tau$, $P_{zz} = P_n$, where P_τ and P_n are the tangential and normal pressure components. The difference between the pressure components at the surface of a macroscopic body gives rise to the surface tension. Similar effect takes place in a shock wave [21]. The surface tension coefficient can be calculated using the formalism [20, 22] as

$$\gamma = \int (P_n - P_\tau) dz.$$

Calculating the pressure components from MD simulation data yields the surface tension coefficient $\gamma = 17.38 = 250$ dynes/cm at $M = 8.19$ and $\gamma = 1.232 = 17.7$ dyne/cm at $M = 2.65$. These results are in qualitative agreement with the estimates [21]. Note that in the case of gases the surface tension is connected with gas kinetic pressure, and the coefficient γ is roughly proportional to $(M^2 - 1)$.

One of the authors (S.A.) is grateful A.I.Larkin for helpful discussions and to the Institute of Laser Engineering, Osaka University for offering the guest position. The work was supported by Russian Fund for Fundamental Research, Grant 95-02-04535a.

1. L.D.Landau and E.M.Lifshitz, *Fluid Mechanics*, Oxford: Pergamon Press, 1959.
2. H.W.Liepman, R.Narashima, and M.T.Chahine, Phys. Fluids **5**, 1313 (1962).
3. D.Gilbarg and D.Paolucci, J. Ratl. Mech. Anal. **2**, 617 (1953).

4. I.E.Tamm, Trudy FIAN (Proc. Lebedev Physical Institute) **29**, 317 (1965).
5. H.M.Mott-Smith, Phys.Rev. **82**, 885 (1951).
6. C.Muckenfuss, Phys.Fluids **5**, 1325 (1962).
7. W.Fiszdon, R.Herczynski, and Z.Walenta, in: *Rarefied Gas Dynamics*, Eds. M.Becker and M.Fiebig, Porz-Wahn, DFVLR Pres, 1974, p.B23
8. S.M.Yen, Ann.Rev.Fluid Mech. **16**, 67 (1984).
9. G.A.Bird, *Molecular Gas Dynamics*, Oxford: Clarendon Press, 1976.
10. G.Ya.Lyubarsky, Sov.Phys.JETP **13**, 740 (1961).
11. R.G.Barantsev, Sov.Phys.JETP **15**, 615 (1962).
12. W.G.Hoover, Phys.Rev.Lett. **42**, 1531 (1979).
13. B.L.Holian, W.G.Hoover, and B.Moran, G.K.Straub, Phys.Rev **A22**, 2798 (1980); B.L.Holian, Phys.Rev. **A37**, 2562 (1988).
14. M.Koshi, T.Saito, H.Nagoya et al., Kayaku Gakkaishi **55**, 229 (1994) (in Japanese).
15. E.Salomons and M.Marechal, Phys.Rev.Lett. **69**, 269 (1992).
16. S.I.Anisimov and V.V.Zhakhovskii, JETP Lett. **57**, 99 (1993).
17. D.W.Heerman, *Computer Simulation Methods in Theoretical Physics*, Berlin – New York: Springer Verlag, 1986.
18. V.V.Zhakhovskii and S.I.Anisimov, JETP **84**, 734 (1997).
19. V.A.Rabinovich, A.A.Vasserman, V.I.Nedostup, and L.S.Veksler, *Thermodynamical Properties of Neon, Argon, Krypton, and Xenon*, Berlin – New York: Hemisphere, 1988.
20. P.Resibois and M.De Lechner, *Classical Kinetic Theory of Fluids*, New York: J.Wiley and Sons, 1977.
21. A.G.Bashkirov, Phys. Fluids **A3**, 960 (1991).
22. J.S.Rowlinson and B.Widom, *Molecular Theory of Capillarity*, Oxford: Clarendon Press, 1982.